Constant Growth Rate Can Be Supported by Decreasing Energy Flux and Increasing Aerobic Glycolysis

Nikolai Slavov,[1,2,3,4,*] Bogdan A. Budnik,[2] David Schwab,[5] Edoardo M. Airoldi,[2,3] and Alexander van Oudenaarden[1,4,*]

[1]Departments of Physics and Biology and Koch Institute for Integrative Cancer Research, Massachusetts Institute of Technology, Cambridge, MA 02139, USA
[2]Department of Statistics and FAS Center for Systems Biology, Harvard University, Cambridge, MA 02138, USA
[3]Broad Institute of MIT and Harvard, Cambridge, MA 02142, USA
[4]Hubrecht Institute, Royal Netherlands Academy of Arts and Sciences and University Medical Center Utrecht, Uppsalalaan 8, 3584 CT Utrecht, the Netherlands
[5]Department of Physics and Lewis-Sigler Institute, Princeton University, Princeton, NJ 08544, USA
*Correspondence: nslavov@alum.mit.edu (N.S.), a.vanoudenaarden@hubrecht.eu (A.v.O.)
http://dx.doi.org/10.1016/j.celrep.2014.03.057

SUMMARY

Fermenting glucose in the presence of enough oxygen to support respiration, known as aerobic glycolysis, is believed to maximize growth rate. We observed increasing aerobic glycolysis during exponential growth, suggesting additional physiological roles for aerobic glycolysis. We investigated such roles in yeast batch cultures by quantifying O_2 consumption, CO_2 production, amino acids, mRNAs, proteins, posttranslational modifications, and stress sensitivity in the course of nine doublings at constant rate. During this course, the cells support a constant biomass-production rate with decreasing rates of respiration and ATP production but also decrease their stress resistance. As the respiration rate decreases, so do the levels of enzymes catalyzing rate-determining reactions of the tricarboxylic-acid cycle (providing NADH for respiration) and of mitochondrial folate-mediated NADPH production (required for oxidative defense). The findings demonstrate that exponential growth can represent not a single metabolic/physiological state but a continuum of changing states and that aerobic glycolysis can reduce the energy demands associated with respiratory metabolism and stress survival.

INTRODUCTION

Understanding cell growth is essential to both basic science and treating diseases associated with deregulated cell growth, such as cancer. Accordingly, cell growth has been studied extensively, from the pioneering work of Krebs and Eggleston (1940) and Monod (1949) to recent discoveries (DeBerardinis et al., 2007; Slavov et al., 2011; Scott et al., 2010; Youk and van Oudenaarden, 2009; Clasquin et al., 2011; Chang et al., 2013). Although the major biochemical networks were identified by the 1950s (Krebs and Eggleston, 1940; Monod, 1949), understanding the coordination between these pathways in time remains a major challenge and opportunity to systems biology (Hartwell et al., 1999; McKnight, 2010; Slavov and Botstein, 2011). The challenge stems from the fact that both cell growth and metabolism may take alternative parallel paths. For example, cells can produce energy either by fermenting glucose to lactate/ethanol to generate two ATP molecules per glucose molecule or by respiration (oxidative phosphorylation) to generate substantially more (between 16 and 36 depending on the estimate) ATP molecules per glucose molecule. The estimates for the in vivo efficiency of oxidative phosphorylation vary widely depending on the measurement method and the underlying assumptions. These estimates come from (1) measuring ATP production during fermentative growth and assuming it equals the ATP production and demand during respiratory growth (von Meyenburg, 1969; Verduyn et al., 1991; Famili et al., 2003), (2) in vivo ^{31}P NMR flux measurements (Campbell et al., 1985; Gyulai et al., 1985; Portman, 1994; Sheldon et al., 1996), and (3) in vitro measurements with isolated mitochondria (Rich, 2003).

Although respiration has higher ATP yield per glucose, cancer/yeast cells tend to ferment most glucose into lactate/ethanol even in the presence of sufficient oxygen to support respiration, a phenomenon known as aerobic glycolysis. This apparently counterintuitive metabolic strategy of using the less efficient pathway is conserved from yeast to human and has been recognized as a hallmark of cancer (Vander Heiden et al., 2009; Hanahan and Weinberg, 2011). Numerous competing models have been proposed to explain aerobic glycolysis both in yeast and in human (Warburg, 1956; Newsholme et al., 1985; De Deken, 1966; Pfeiffer et al., 2001; Gatenby and Gillies, 2004; Molenaar et al., 2009; Vander Heiden et al., 2009; Vazquez et al., 2010; Shlomi et al., 2011; Lunt and Vander Heiden, 2011; Ward and Thompson, 2012).
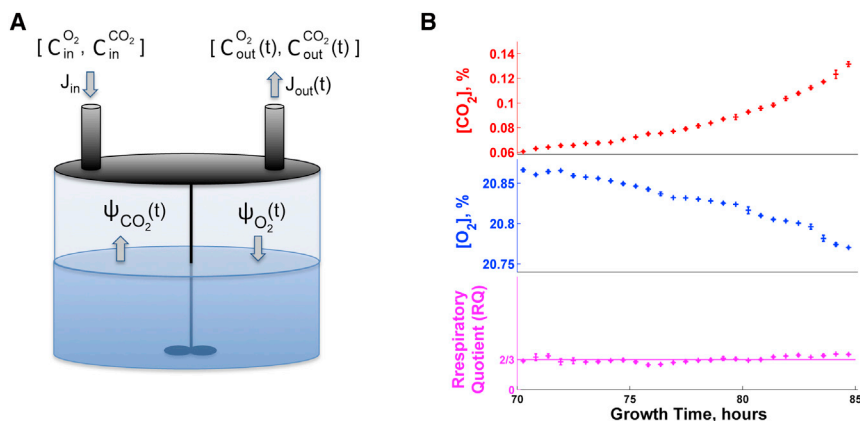
Figure 1. Experimental Design for Precision Measurements of O_2 Uptake and CO_2 Production in Time

(A) A conceptual schematic of the method used for precision measurements of O_2 and CO_2 fluxes in low-density yeast cultures; C_{in} are the concentrations of gases in the air entering the reactor at rate J_{in}, and the C_{out} are the concentrations of gases existing the reactor at rate J_{out}.

(B) The respiratory quotient (RQ) estimated from O_2 and CO_2 concentrations measured in a low-density yeast culture growing on ethanol as a sole source of carbon and energy equals the RQ estimate from mass conservation (2/3); the culture was inoculated at a density of 1,000 cells/ml, and measurements began 70 hr after inoculation, when the culture had reached a density of about 10^5 cells/ml.

Error bars denote SDs. See Figure S1 and the Supplemental Information for more control experiments and details.

Although the models propose different and often conflicting mechanisms, they aim to explain aerobic glycolysis as a metabolic strategy for maximizing the cellular growth rate. However, in some cases slowly growing or even quiescent cells exhibit aerobic glycolysis (Boer et al., 2008; Lemons et al., 2010; Slavov and Botstein, 2013). Theoretical models of aerobic glycolysis are limited by the many incompletely characterized tradeoffs of respiration and fermentation, such as the effects of aerobic glycolysis on signaling mechanisms (Chang et al., 2013). Further limitations stem from missing estimates for key metabolic fluxes. For example, depending on whether the increase in the flux of fermented glucose compensates for the low efficiency of fermentation, aerobic glycolysis may either increase or decrease the rate of energy (ATP) production. To better understand the role of aerobic glycolysis for cell growth, we sought to measure directly and precisely the fluxes of O_2 consumption and CO_2 production, and gene regulation (including levels of mRNAs, proteins, and posttranslational modifications) in the conditions of aerobic glycolysis and exponential growth.

RESULTS

Rates of O_2 consumption and CO_2 production have been measured (von Meyenburg, 1969; Verduyn et al., 1991; Van Hoek et al., 1998, 2000; Jouhten et al., 2008; Wiebe et al., 2008) in high-density yeast cultures growing in chemostats at steady state. The most commonly used laboratory growth condition, low-density cultures growing in a batch, however, is a challenging condition for measuring O_2 consumption and CO_2 production because the small number of rapidly growing cells results in small and rapidly changing fluxes. To overcome this challenge and quantify the relative importance of respiration and fermentation during batch cell growth, we developed a bioreactor in which we can accurately measure the absolute rates of O_2 uptake (Ψ_{O_2}) and CO_2 synthesis (Ψ_{CO_2}). In this setup (Figure 1A), a constant flow of air at rate J_{in} containing 20.9% O_2 and 0.04% CO_2 is fed into the bioreactor. By accurately measuring, every second, the O_2 and CO_2 concentrations in

the gas leaving the reactor and applying mass conservation (Equations 1 and 2), we can estimate Ψ_{O_2} and Ψ_{CO_2}:

$$\psi_{O_2}(t) = \frac{1}{V_m}\left[J_{in}C_{in}^{O_2} - J_{out}(t)C_{out}^{O_2}(t)\right] \quad \text{(Equation 1)}$$

$$\psi_{CO_2}(t) = \frac{1}{V_m}\left[J_{in}C_{in}^{CO_2} - J_{out}(t)C_{out}^{CO_2}(t)\right] \quad \text{(Equation 2)}$$

The fluxes are normalized to moles per hour by the molar volume V_m of air at 25°C and 1 atmosphere. The outflow rate (J_{out}) is determined from mass balance analysis and is typically very similar to J_{in}; see Supplemental Information.

To evaluate the accuracy of the O_2 and CO_2 fluxes, we measured these fluxes in control growth conditions for which the molar ratio of CO_2 to O_2, known as respiratory quotient (RQ), is known. First, we grew cells in media containing 100 mM ethanol as a sole source of carbon and energy. The complete oxidation of an ethanol molecule requires three O_2 molecules and produces two CO_2 molecules; thus, chemical stoichiometry and mass conservation require that the RQ for ethanol oxidation equals 2/3, providing a strong benchmark for evaluating the accuracy of our measurements. The measured RQ (Figure 1B) matches the expected value of 2/3. Importantly, the sensitivity of our sensors to very small changes both in O_2 consumption (0.005%) and CO_2 production (0.002%) allows measuring fluxes from low-density yeast cultures (10^5 cells/ml); see Supplemental Information and Figure S1 for details and more control experiments.

Growth Rate and Doubling Time Remain Constant for Nine Doublings

Having established a system for accurate quantification of O_2 and CO_2 fluxes, we applied it to a batch culture of budding yeast; 2 l of well-aerated and well-stirred minimal medium containing 11.11 mM glucose as a sole source of carbon and energy were inoculated to a cell density of 1,000 cells/ml; see Supplemental Information. After 10 hr, the culture reached a cell density allowing bulk measurements and was continuously sampled (Figures 2A and S2). During the first 15 hr of sampling (nine doubling
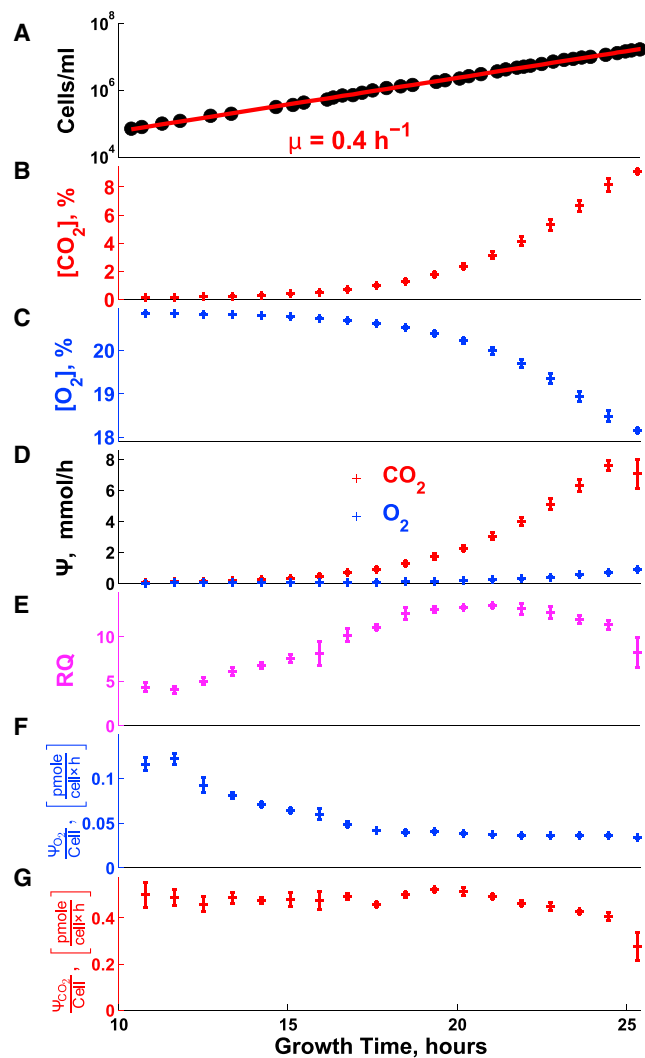
Figure 2. Rates of Respiration and Fermentation Evolve Continuously during Batch Growth at a Constant Growth Rate

(A) Cell density (single cells per ml) during exponential growth on glucose as a sole source of carbon and energy.

(B) The levels of O_2 in the exhaust gas were measured continuously (every second) with a ZrO_2 electrochemical cell.

(C) The levels of CO_2 in the exhaust gas were measured continuously (every second) with infrared spectroscopy.

(D) Fluxes of O_2 uptake (Ψ_{O_2}) and CO_2 production (Ψ_{CO_2}) estimated from the data in (B) and (C) and Equations 1 and 2; see Supplemental Information for details.

(E) Respiratory quotient (RQ), defined as the ratio of Ψ_{CO_2} to Ψ_{O_2}.

(F) Rate of O_2 uptake per cell.

(G) Rate of CO_2 production per cell.

In all panels, error bars denote SDs. See also Figure S2.

periods, the pink region in Figure S2), the cell density increased exponentially with time, indicating a constant rate of cell division ($\mu = 0.4$ hr^{-1}, 1.7 hr doubling time), followed by sudden and complete cessation of growth and division upon glucose exhaustion. Then the cells resumed growth (purple region in Figure S2) supported by the ethanol accumulated during the first growth phase. Notably, during the second growth phase,

biomass increased exponentially, indicating again a constant but much slower growth rate $\mu = 0.04$ hr^{-1}. Thus, our experimental design provides two phases of exponential growth, characterized by different carbon sources and growth rates. The transition between the two phases has been studied extensively (Brauer et al., 2005; Zampar et al., 2013), and we will not address it; rather, we focus only on the phases with constant doubling times.

Oxygen Uptake Decreases during Growth at a Constant Rate

The continuously measured concentrations of O_2 and CO_2 (Figures 2B and 2C), and the fluxes estimated from them (Figure 2D), allow computing the RQ during the first phases of exponential growth (Figure 2E). Because the complete oxidation of a glucose molecule requires six O_2 and produces six CO_2, RQ >1 indicates that some glucose is also fermented in the presence of high level of O_2 (Figure 2B), i.e., aerobic glycolysis. Such aerobic glycolysis (RQ >1; Figure 2E) and the exponential growth in Figure 2A are consistent with previous observations (Brauer et al., 2005; Zampar et al., 2013) and expectations. In stark contrast, the continuously changing metabolic fluxes per cell (Figures 2E and 2F) during exponential growth suggest that the cells may not be at steady state even when their growth rate remains constant; this observation is so unexpected that we sought to test it further by multiple independent experimental measurements described below. A second surprising observation is the direction of change: as cells grow and deplete glucose, the oxygen consumption per cell decrease (Figure 2F). This decreasing respiration likely contributes to the cessation of growth after the first growth phase (Figure S2) because cells with downregulated respiration are challenged to grow on ethanol, an obligatory respiratory condition. During the last doublings on glucose, RQ remains high, albeit beginning to decline in concert with CO_2 (Figures 2E and 2G), indicating that the metabolism remains mostly fermentative as long as glucose is present in the medium.

We sought to further test, by independent measurements and mass conservation, the dynamically evolving rates of respiration and fermentation (Figures 2E and 2F) quantified during exponential growth. During the entire first growth phase (Figure 3A), we evaluated whether the flux of carbon intake from glucose equals the sum of all major output carbon fluxes (those due to respiration, biomass synthesis, and fermentation), as required by mass conservation. The results of this mass-balance analysis (Figure 3B) demonstrate that the carbon fluxes estimated from the biomass and the gas measurements account completely and accurately for the fluxes estimated from glucose uptake, thus confirming the accuracy of all measurements and the metabolic dynamics at a constant doubling time.

ATP Production and Stress Resistance Decrease during Exponential Growth

Increasing the rate of aerobic glycolysis is often modeled as a metabolic requirement for increasing the rate of growth (Newsholme et al., 1985; Pfeiffer et al., 2001; Molenaar et al., 2009; Vander Heiden et al., 2009; Vazquez et al., 2010; Shlomi et al., 2011; Lunt and Vander Heiden, 2011; Ward and Thompson, 2012). Because the growth rate remains constant during the
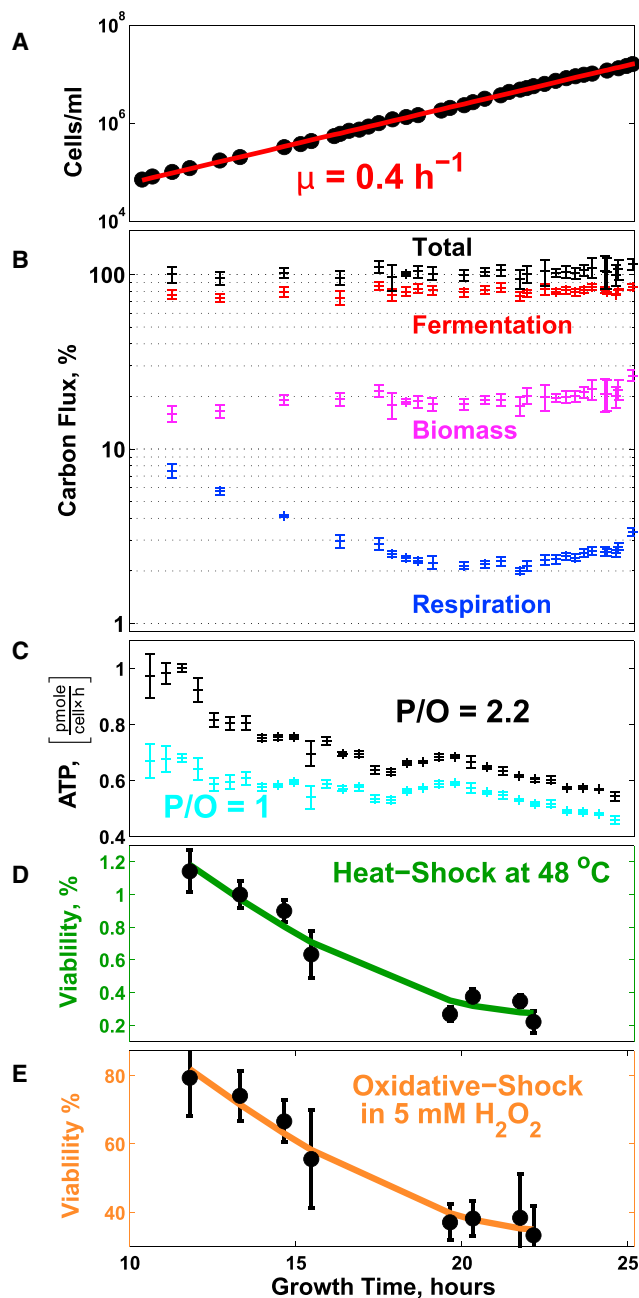
Figure 3. The Fraction of Glucose Carbon Flux Incorporated into Biomass and the Sensitivity to Stress Increase while the Growth Rate Remains Constant

(A) Exponential increase in the number of cells indicates a constant doubling period.

(B) The fraction of carbon flux from glucose (moles of carbon per hour) directed into the major metabolic pathways, as computed from the gas and biomass data, evolves continuously; the sum of the fluxes through these pathways (total) can account, at all time points, for the carbon intake flux from glucose; see Supplemental Information.

(C) The ATP flux was estimated from the fluxes of CO_2 and O_2 in Figures 2E and 2F for low efficiency of oxidative phosphorylation, 1 ATP per oxygen atom (16 ATPs/glucose), and for high efficiency, 2.2 ATPs per oxygen atom (30.4 ATPs/ glucose).

exponential growth phase (Figures 2A and 3A), maximizing growth rate cannot be the only factor accounting for the increasing rate of aerobic glycolysis that we measured (Figures 2E and 3B). Other factors must also influence the rate of aerobic glycolysis.

The reduced oxygen consumption per cell (Figure 2F) and the slight increase in the fraction of glucose carbon directed to biomass synthesis (Figure 3B) suggest a hypothesis, namely, that the increasing rate of aerobic glycolysis might reduce the ATP flux, whereas the cells maintain the same growth rate. To test this hypothesis, we used the O_2 and CO_2 fluxes (Figure 2C) to estimate the rate of ATP production over the range of reported efficiency of oxidative phosphorylation (Hinkle, 2005); see Supplemental Information. The result suggests decreasing rates of total ATP production (Figure 3C), bolstering our hypothesis. The declines in respiration (Figure 2F) and ATP flux (Figure 3C) parallel declines in both heat and oxidative stress resistance (Figures 3D and 3E). In contrast to previous reports (Lu et al., 2009; Zakrzewska et al., 2011), we observe changes in stress resistance, whereas the growth rate remains constant. If the rate of ATP production reflects the cellular energetic demands (Famili et al., 2003), the decreasing ATP flux likely reflects the energy demands associated with respiratory metabolism and stress survival. Thus, the reduced respiration during aerobic glycolysis can reduce the overall rate of energy production (likely reflecting energy demands) in cells maintaining a constant growth rate.

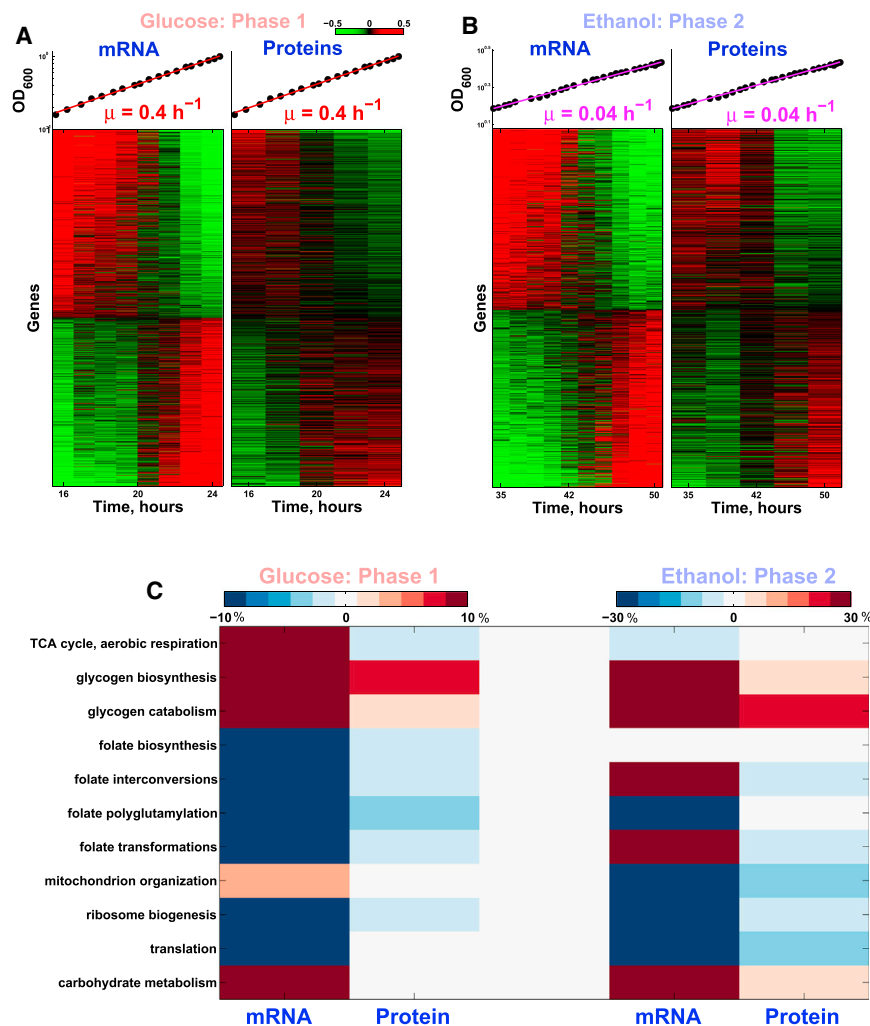## Global Remodeling of Gene Regulation during Exponential Growth

To further evaluate the extent of the metabolic remodeling at a constant doubling period and to identify its molecular basis, we measured the levels of both mRNAs and proteins during the two phases of exponential growth, on glucose or on ethanol (Figure 4). Proteins were labeled with tandem mass tags (TMTs) and quantified by mass spectrometry (MS), resulting in over 58,000 quantified distinct peptides corresponding to over 5,000 proteins at a false discovery rate (FDR) <1%. The peptides where quantified at MS2 level, resulting in high reproducibility (Spearman ρ = 0.993 for swapped TMT labels; Figure S4A) and reliable estimates of fold changes (error <30%) as verified from measuring the levels of the dynamic universal proteomics standard (UPS2) spiked into the yeast samples (Figure S4B). The accuracy of UPS2 fold changes was highest for peptides with low coisolation inferences and thus quantifying proteins based only on peptides with low coisolation improves the accuracy.

During each exponential growth phase, over 1,000 genes (at FDR <1%) increase or decrease monotonically at both the mRNA and the protein levels (Figures 4A and 4B); these genes are highly enriched (Bonferroni corrected p values < 10^{-42}) for

(D) The ability of the cells to survive heat shock (48°C for 10 min) declines during the exponential growth phase. Stress sensitivity was quantified by counting colony-forming units (CFUs) on YPD plates.

(E) The ability of the cells to survive oxidative-shock (5 mM H_2O_2 for 10 min) declines during the exponential growth phase.

In all panels, error bars denote SDs. See also Figure S3.

Figure 4. Global Remodeling of mRNA and Protein Regulation during Batch Growth at a Constant Growth Rate

(A) Thousands of mRNAs and proteins (FDR <1%) either increase or decrease monotonically in abundance during the first phase of exponential growth. Levels are reported on a $\log_2$ scale with a 2-fold dynamic range. The mRNA and protein levels were measured in independent (biological replica) cultures, and their correlation reflects the reproducibility of the measurements.

(B) Thousands of mRNAs and proteins (FDR <1%) either increase or decrease monotonically in abundance during the second phase of exponential growth.

(C) Metabolic pathways that show statistically significant dynamics (FDR <1%) during the two phases of exponential growth; see Supplemental Information. The magnitude of change for each gene set is quantified as the average percentage change in the level of its genes per doubling period of the cells.

See also Figure S4.

acid biogenesis (Gcn4p, Fhl1p, Leu3p, Arg81p, Met4p, and Met32p) and ribosomal biogenesis (Fhl1p, Sfp1p, and Rap1p). The genes whose mRNA levels increase during the exponential growth phase overlap significantly with the targets of TFs regulating cell division (Fkh2p), stress response (Msn2p, and Msn4p), and redox metabolism (Aft1p and Aft2p). The functions and the changing activities of these TFs mirror the transcriptional responses from which they are inferred and add a layer of mechanistic detail to the regulatory dynamics during exponential growth at a constant rate.

metabolic and protein synthesis functions (see Supplemental Information), emphasizing the global restructuring of metabolism even as the growth rate remains constant. A decline in protein synthesis genes has been observed previously during the last doubling before glucose exhaustion (Ju and Warner, 1994), and our data show that such decline begins much earlier and continues over many doublings at a constant rate.

Transcription Factors Mediating the Transcriptional Response

The changes in mRNA levels that we measured during exponential growth could reflect two regulatory mechanisms, changes in mRNA production and/or degradation rates. To identify transcription factors (TFs) that mediate some of the changes in the rate of mRNA transcription, we overlapped known TF target genes (MacIsaac et al., 2006) with the sets of genes that either increase or decrease during the first phase of exponential growth (FDR <1%); see Supplemental Information. The results (Table S1) indicate very significant overlap between the genes whose mRNAs decline and the targets of TFs involved in amino

Dynamics of Enzymes Regulating Respiratory Metabolism

During the two phases of exponential growth, we systematically compared the dynamic trends in mRNA and protein levels for gene sets defined by all annotated biochemical pathways and by the gene ontology (GO). The statistical significance of the trends within a pathway, quantified by regression slopes, was evaluated by bootstrapping (Airoldi et al., 2009); see Supplemental Information and Figures S4C and S4D for details and all significant genes sets at FDR <1%. Among the pathways exhibiting significant dynamics are gene sets (Figure 4C) mediating the measured changes in metabolic fluxes (Figure 2). The decline in the fraction of aerobically metabolized glucose (Figure 3B) and oxygen consumption (Figure 2F) parallels a decline in the key enzymes that funnel metabolites to respiration. These enzymes include the carnitine shuttle enzymes (Cat2p, Yat1p, and Yat2p) that feed acetyl-CoA to the tricarboxylic acid (TCA) cycle and the rate-regulatory TCA cycle enzymes (Figures 5A and S4)
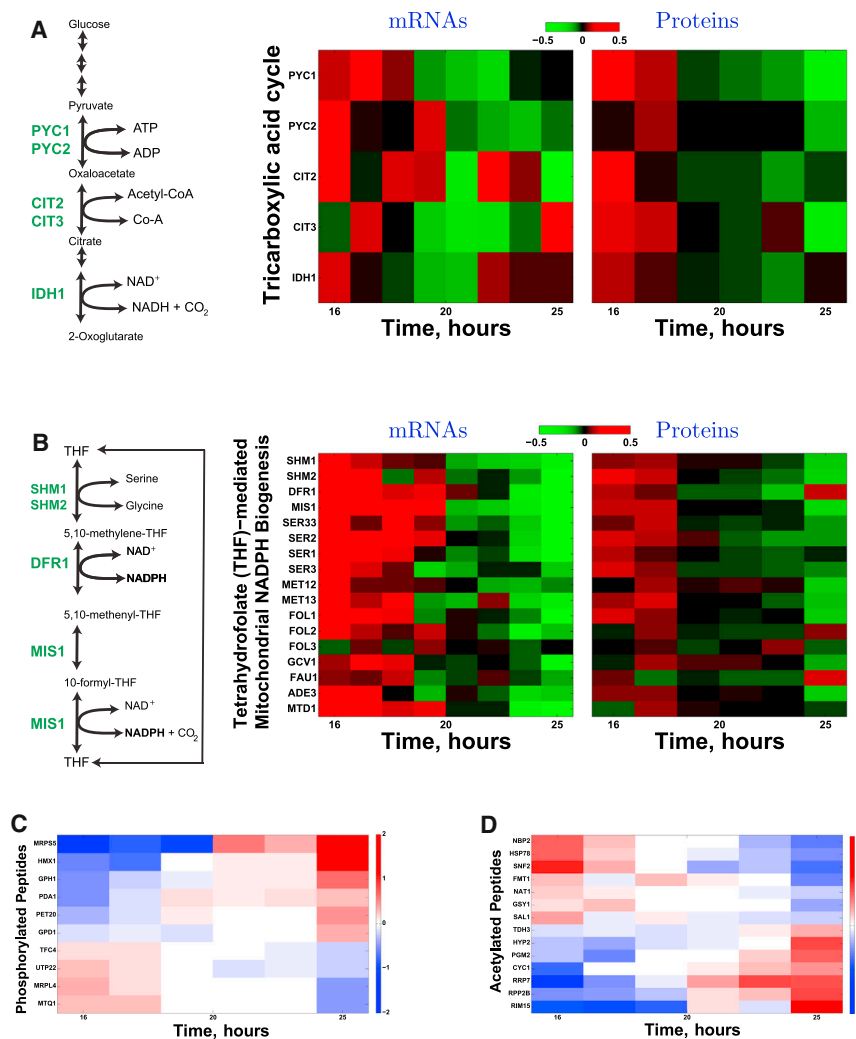
Figure 5. Dynamics of Enzymes and Post-translational Modifications Regulating Respiratory Metabolism at a Constant Growth Rate

(A) The levels of enzymes (and their corresponding mRNAs) catalyzing the first rate-determining reactions of the tricarboxylic acid (TCA) cycle decline, parallel to the decreased oxygen consumption (Figure 2F), during the first exponential growth phase. These enzymes include the pyruvate carboxylases (Pyc1p and Pyc2p), citrate synthetases (Cit1p and Cit2p), and the isocitrate dehydrogenase (Idh1p). See Figures 4 and S4 for other related pathways that also show statistically significant declines. The data are displayed on a $\log_2$ scale with 2-fold dynamical range.

(B) The levels of enzymes (and their corresponding mRNAs) catalyzing the tetrahydrofolate (THF)-mediated mitochondrial NADPH biogenesis decline, parallel to the decreased oxygen consumption (Figure 2F), during the first exponential growth phase. These include all enzymes (Ser3p, Ser33p, Ser1p, and Ser2p) catalyzing the serine biosynthesis from 3-phosphoglycerate, the hydroxymethyltransferases (Shm1p and Shm2p) and the mitochondrial NADPH synthetases: the dihydrofolate reductase (Dfr1p) and the mitochondrial C1-tetrahydrofolate synthase (Mis1p). See Figures 4 and S4 for other related pathways that also show statistically significant declines. The data are displayed on a $\log_2$ scale with 2-fold dynamical range.

(C) Levels of phosphorylated peptides change during exponential growth at a constant rate.

(D) Levels of acetylated peptides change during exponential growth at a constant rate. The levels of peptides with posttranslational modifications are shown on a $\log_2$ scale, and the corresponding proteins are marked on the y axis.

See also Figure S5.

that catalyze the reactions through which metabolites enter the TCA. The levels of some mRNAs coding for TCA enzymes also decrease, whereas the levels of other mRNAs coding for TCA enzymes increase (Figure S5A). The levels of mRNAs coding for the initial and flux-regulatory TCA enzymes decline in concert with the corresponding proteins, including pyruvate carboxylase (PYC) isoforms 1 and 2, citrate synthetases 2 and 3, and the isocitrate dehydrogenase 1 (Figure 5A). Another transcriptional reflection of the decreased respiration during phase 1 is the decline of the mRNAs for the glutathione-dependent oxidoreductases (GRX3 and GRX4; Figure S5B), whose transcription is sensitive to peroxide and superoxide radicals (Pujol-Carrion et al., 2006).

The mitochondrial respiratory chain generates reactive oxygen species (ROS) whose neutralization requires tetrahydrofolate (THF)-mediated mitochondrial NADPH production from the carbon 3 of serine by the reactions shown in Figure 5B (Appling, 1991; García-Martínez and Appling, 1993). All enzymes (and their corresponding mRNAs) producing NADPH from these pathways and from the associated pathways (Figures 5B and S4) decline in parallel with the declining oxygen

consumption (Figure 2) during the exponential growth phase. This concerted decline is particularly pronounced for the mitochondrial enzymes (Dfr1p and Mis1p) catalyzing the NADPH generating reactions (Figure 5B). The decline also includes all enzymes (Ser3p, Ser33p, Ser1p, and Ser2p) catalyzing the serine biosynthesis from 3-phosphoglycerate. Because the growth rate and the cytoplasmic serine concentration remain constant (Figure S5C), the declining levels of serine biosynthetic enzymes likely reflect a decreasing flux of serine toward the folate-mediated mitochondrial NADPH production. Such a decrease in NADPH production could explain at least in part the decreased stress resistance that we measured (Figures 3D and 3E). This pathway for THF-mediated mitochondrial NADPH production is transcriptional upregulated with the growth rate and increased respiration of yeast growing on ethanol carbon source (Slavov and Botstein, 2011), suggesting its broader significance for respiratory metabolism.

Similarly, pervasive dynamics in metabolic pathways are observed during the second phase of exponential growth (Figure 4C and Figure S4C). The changing levels of metabolic enzymes synthesizing amino acids during the two exponential

OPEN
ACCESS
CellPress

phases also lead to concerted changes in the intracellular amino acid levels (Figure S5C).

Posttranslational Modifications during Exponential Growth

Hundreds of peptides quantified by MS carried posttranslational modifications (PTMs), such as phosphorylation (of Ser and Thr) and acetylation (of Lys and Arg). Similar to the metabolic fluxes, mRNA and protein levels, the levels of peptides with PTMs increase or decrease over 10-fold dynamic range (Figures 5C, 5D, and S5D) during the exponential growth phases. These PTM dynamics reinforce the regulatory dynamics suggested by the metabolic fluxes, mRNAs, and proteins levels (Figures 4A and 4B). For example, the decreasing fraction of glucose carbon directed toward respiration is associated with the phosphorylation of the pyruvate dehydrogenase (Pda1p) that regulates the balance between respiration and fermentation and the acetylation of the glycolytic enzyme glyceraldehyde-3-phosphate dehydrogenase (Tdh3p). Furthermore, the reduced respiration per cell (Figure 2F) is reflected in the phosphorylation pattern (Figure 5C) of mitochondrial respiratory and heme-related proteins (Pet20p and Hmx1p), of mitochondrial ribosomal proteins (Mrps5p and Mrpl4p), and the acetylation pattern (Figure 5D) of Cytochrome c (Cyc1p). The increasing metabolism of reserved carbohydrates during the first growth phase indicated by the mRNA and protein trends (Figures 4A–4C and S4) is also detected in the PTMs of participating enzymes (Gph1p and Pgm2p). Similarly, the translation-related changes in gene regulation (Figures 4A–4C and S4) are paralleled by translation-related PTMs including proteins involved in rRNA maturation and ribosome biogenesis (Utp22p and Rrp7p), elongation-related factors (Hyp2p, Rpp2bp, and Mtq1p), and tRNA synthesis (Tfc4p). Other proteins with dynamic PTMs during exponential growth (Figures 5C and 5D) include the proliferation regulating kinase Rim15p, the acetyltransferase (Nat1p), and the methyltransferase (Mtq1p), suggesting crosstalk among PTM signaling pathways. These results imply that quantifying PTM dynamics during well-characterized physiological states is a promising direction for characterizing the vast and largely unexplored space of PTM functions.

DISCUSSION

Six independent measurements (respiration, stress resistance, transcripts, proteins, amino acids, and PTMs) demonstrate that metabolism, gene regulation, and stress sensitivity can change substantially even when the doubling time does not change over nine generations. Specifically, we found that, as aerobic glycolysis increases, a constant rate of biomass synthesis can be sustained with decreasing rate of ATP production. In other words, cells with reduced rate of respiration are able to maintain their growth rate constant with lower total ATP flux. Thus, if the rate of ATP production reflects the cellular energy demands (Famili et al., 2003), our data suggest that although respiration is efficient in generating ATP, it may also substantially increase the energetic demands for growth, even when growth rate remains constant for many generations. Therefore, aerobic glycolysis may reduce the energetic demands of cellular growth by

reducing the energy associated with respiration, such as that needed for detoxification of reactive oxygen species. Such decreased oxidative-stress defenses can naturally explain the decreasing stress resistance that we measured in the course of exponential growth at a constant rate.

The decreasing rate of ATP production with the shift toward less aerobic metabolism prompts the reevaluation of the current estimates for the efficiency of oxidative phosphorylation based on the assumption that yeast growing in aerobic and in anaerobic conditions have identical energy requirements (von Meyenburg, 1969; Verduyn et al., 1991; Famili et al., 2003). The decreased respiration in our cultures coincides with a concerted downregulation, at both the mRNA and protein levels, of the TCA enzymes regulating the entry of metabolites into the respiratory pathway. This downregulation of rate-determining enzymes not only supports the measured decrease in oxygen consumption but also suggests the molecular mechanisms mediating it. Similarly, we found that all pathways associated with the tetrahydrofolate-mediated production of mitochondrial NADPH decline in parallel to the decreased oxygen consumption and the decreased stress resistance, emphasizing the ROS burden of respiratory metabolism and the role of mitochondrial NADPH for relieving it.

Most work on aerobic glycolysis has focused on the correlation between aerobic glycolysis and growth rate (Warburg, 1956; Newsholme et al., 1985; De Deken, 1966; Brand and Hermfisse, 1997; Pfeiffer et al., 2001; Bauer et al., 2004; Gatenby and Gillies, 2004; Molenaar et al., 2009; Vander Heiden et al., 2009; Vazquez et al., 2010; Shlomi et al., 2011; Lunt and Vander Heiden, 2011; Ward and Thompson, 2012). However, there are also examples of decoupling aerobic glycolysis and growth rate. These examples include high rates of fermentation measured in slowly growing yeast whose growth is limited by auxotrophic nutrients (Boer et al., 2008; Slavov and Botstein, 2013) and in quiescent mammalian fibroblasts whose growth is inhibited by serum withdrawal and/or contact inhibition (Lemons et al., 2010). Our data and analysis build upon and expand previous work showing decoupling of aerobic glycolysis and cellular growth rate in several ways: (1) measurements of oxygen consumption (Figure 2), (2) estimation of the total rate of ATP production (Figure 3), (3) demonstration that the measured flux of carbon intake equals the measured flux of carbon release (Figure 3), (4) measurements of stress resistance (Figure 3), and (5) measurements of protein levels and PTMs (Figures 4 and 5). The measurement of oxygen consumption allows quantifying the extent of aerobic glycolysis by the respiratory quotient, and the carbon flux balance provides a cross-check of all measurements. Thus, we can rule out the possibility that our results are influenced by unmeasured fluxes, such as respiration, or by incorrectly measured fluxes. Our results are also unlikely to be influenced by mutations and external perturbations because our measurements were performed in wild-type cells growing in very well-defined conditions. The estimate of energy production indicates that cells can support a constant growth rate while decreasing the rate of energy production and increasing the rate of aerobic glycolysis. Our results are consistent with and add to previous work (Brand and Hermfisse, 1997; Lemons et al., 2010; Jain et al., 2012; Chang et al., 2013)

pointing to roles of aerobic glycolysis beyond maximizing cellular growth rate. Therefore, we conclude that understanding aerobic glycolysis requires taking into account multiple aspects of aerobic metabolism, such as mitochondrial NADPH production, not just the growth rate.

Many researchers (Ju and Warner, 1994; Shachrai et al., 2010; Zampar et al., 2013; Bren et al., 2013) have reported dynamic changes during batch growth. To our knowledge, all previous reports were confined either to nonexponentially growing cultures or to a single exogenous protein or to the last generation of batch growth when growth rate, to the extent it can estimated, was declining. In contrast, we observed pervasive dynamics during the whole span (including early and middle phases) of batch growth, including during phases that are considered to represent a single well-defined steady state (Newman et al., 2006; Belle et al., 2006; Pelechano and Pérez-Ortín, 2010; Schwanhäusser et al., 2011; Heyland et al., 2009; Youk and van Oudenaarden, 2009; Boisvert et al., 2012).

Our data demonstrate that, at least for two very different growth conditions, exponentially growing cultures can change their metabolism continuously, prompting the investigation of metabolic and cell-signaling dynamics even in conditions previously assumed to represent steady states (Silverman et al., 2010; Slavov et al., 2011, 2013). However, our data do not suggest that all exponentially growing cultures change their metabolism continuously and steady state is impossible; many examples document constant, steady-state fluxes in exponentially growing cultures (von Meyenburg, 1969; Küenzi and Fiechter, 1969; Van Hoek et al., 2000; Brauer et al., 2005, 2008; Slavov and Botstein, 2011, 2013). Our finding of changing metabolism and cell physiology at a constant growth rate provides a new direction for studying physiological dynamics and tradeoffs, such as allowing flux-balance models to account for a constant growth rate at varying glucose uptake rates.

EXPERIMENTAL PROCEDURES

All experiments described in the paper used a prototrophic diploid strain (DBY12007) with a S288c background and wild-type HAP1 alleles, MATa/MATα HAP 1^+. We grew our cultures in a commercial bioreactor (LAMBDA Laboratory Instruments), using minimal media with the composition of yeast nitrogen base (YNB) supplemented with 2 g/l D-glucose. CO_2 and O_2 were measured, every second, in the off-gas with zirconia and infrared sensors, respectively. All other measurements were done on samples taken from the culture via a sterile sampling port. Cell density was measured by a Coulter counter counting of at least 20,000 cells (Slavov et al., 2011; Bryan et al., 2012). Stress sensitivity was assayed (Slavov et al., 2012) by exposing 250 μl culture to stress for 10 min and subsequent plating on YPD plates to count colony forming units (survived cells). Details for all measurements and quality controls can be found in the Supplemental Information.

ACCESSION NUMBERS

The GEO accession number for the gene expression data reported herein is GSE56773.

SUPPLEMENTAL INFORMATION

Supplemental Information includes Supplemental Experimental Procedures, five figures, one table, and one data file and can be found with this article online at http://dx.doi.org/10.1016/j.celrep.2014.03.057.

REFERENCES

Airoldi, E.M., Huttenhower, C., Gresham, D., Lu, C., Caudy, A., Dunham, M., Broach, J., Botstein, D., and Troyanskaya, O.G. (2009). Predicting cellular growth from gene expression signatures. PLoS Comput. Biol., e1000257.

Appling, D.R. (1991). Compartmentation of folate-mediated one-carbon metabolism in eukaryotes. FASEB J. 5, 2645–2651.

Bauer, D.E., Harris, M.H., Plas, D.R., Lum, J.J., Hammerman, P.S., Rathmell, J.C., Riley, J.L., and Thompson, C.B. (2004). Cytokine stimulation of aerobic glycolysis in hematopoietic cells exceeds proliferative demand. FASEB J. 18, 1303–1305.

Belle, A., Tanay, A., Bitincka, L., Shamir, R., and O'Shea, E.K. (2006). Quantification of protein half-lives in the budding yeast proteome. Proc. Natl. Acad. Sci. USA 103, 13004–13009.

Boer, V.M., Amini, S., and Botstein, D. (2008). Influence of genotype and nutrition on survival and metabolism of starving yeast. Proc. Natl. Acad. Sci. USA 105, 6930–6935.

Boisvert, F.-M., Ahmad, Y., Gierliński, M., Charrière, F., Lamont, D., Scott, M., Barton, G., and Lamond, A.I. (2012). A quantitative spatial proteomics analysis of proteome turnover in human cells. Mol. Cell. Proteomics 11, 011429.

Brand, K.A., and Hermfisse, U. (1997). Aerobic glycolysis by proliferating cells: a protective strategy against reactive oxygen species. FASEB J. 11, 388–395.

Brauer, M.J., Saldanha, A.J., Dolinski, K., and Botstein, D. (2005). Homeostatic Adjustment and Metabolic Remodeling in Glucose-limited Yeast Cultures. Molecular Biology of the Cell 16, 2503–2517, 19.

Brauer, M.J., Huttenhower, C., Airoldi, E.M., Rosenstein, R., Matese, J.C., Gresham, D., Boer, V.M., Troyanskaya, O.G., and Botstein, D. (2008). Coordination of growth rate, cell cycle, stress response, and metabolic activity in yeast. Mol. Biol. Cell 19, 352–367.

Bren, A., Hart, Y., Dekel, E., Koster, D., and Alon, U. (2013). The last generation of bacterial growth in limiting nutrient. BMC Syst. Biol. 7, 27.

Bryan, A.K., Engler, A., Gulati, A., and Manalis, S.R. (2012). Continuous and long-term volume measurements with a commercial Coulter counter. PLoS ONE 7, e29866.

Campbell, S.L., Jones, K.A., and Shulman, R.G. (1985). In vivo 31P nuclear magnetic resonance saturation transfer measurements of phosphate exchange reactions in the yeast Saccharomyces cerevisiae. FEBS Lett. 193, 189–193.

Chang, C.-H., Curtis, J.D., Maggi, L.B., Jr., Faubert, B., Villarino, A.V., O'Sullivan, D., Huang, S.C., van der Windt, G.J., Blagih, J., Qiu, J., et al. (2013). Posttranscriptional control of T cell effector function by aerobic glycolysis. Cell 153, 1239–1251.

Clasquin, M.F., Melamud, E., Singer, A., Gooding, J.R., Xu, X., Dong, A., Cui, H., Campagna, S.R., Savchenko, A., Yakunin, A.F., et al. (2011). Riboneogenesis in yeast. Cell 145, 969–980.

De Deken, R.H. (1966). The Crabtree effect: a regulatory system in yeast. J. Gen. Microbiol. 44, 149–156.

DeBerardinis, R.J., Mancuso, A., Daikhin, E., Nissim, I., Yudkoff, M., Wehrli, S., and Thompson, C.B. (2007). Beyond aerobic glycolysis: transformed cells can

engage in glutamine metabolism that exceeds the requirement for protein and nucleotide synthesis. Proc. Natl. Acad. Sci. USA *104*, 19345–19350.

Famili, I., Förster, J., Nielsen, J., and Palsson, B.O. (2003). Saccharomyces cerevisiae phenotypes can be predicted by using constraint-based analysis of a genome-scale reconstructed metabolic network. Proc. Natl. Acad. Sci. USA *100*, 13134–13139.

García-Martínez, L.F., and Appling, D.R. (1993). Characterization of the folate-dependent mitochondrial oxidation of carbon 3 of serine. Biochemistry *32*, 4671–4676.

Gatenby, R.A., and Gillies, R.J. (2004). Why do cancers have high aerobic glycolysis? Nat. Rev. Cancer *4*, 891–899.

Gyulai, L., Roth, Z., Leigh, J.S., Jr., and Chance, B. (1985). Bioenergetic studies of mitochondrial oxidative phosphorylation using 31phosphorus NMR. J. Biol. Chem. *260*, 3947–3954.

Hanahan, D., and Weinberg, R.A. (2011). Hallmarks of cancer: the next generation. Cell *144*, 646–674.

Hartwell, L.H., Hopfield, J.J., Leibler, S., and Murray, A.W. (1999). From molecular to modular cell biology. Nature *402* (6761, Suppl), C47–C52.

Heyland, J., Fu, J., and Blank, L.M. (2009). Correlation between TCA cycle flux and glucose uptake rate during respiro-fermentative growth of Saccharomyces cerevisiae. Microbiology *155*, 3827–3837.

Hinkle, P. (2005). P/O ratios of mitochondrial oxidative phosphorylation. Biochimica et Biophysica Acta (BBA)-. Bioenergetics *1706*, 1–11.

Jain, M., Nilsson, R., Sharma, S., Madhusudhan, N., Kitami, T., Souza, A.L., Kafri, R., Kirschner, M.W., Clish, C.B., and Mootha, V.K. (2012). Metabolite profiling identifies a key role for glycine in rapid cancer cell proliferation. Science *336*, 1040–1044.

Jouhten, P., Rintala, E., Huuskonen, A., Tamminen, A., Toivari, M., Wiebe, M., Ruohonen, L., Penttilä, M., and Maaheimo, H. (2008). Oxygen dependence of metabolic fluxes and energy generation of Saccharomyces cerevisiae CEN.PK113-1A. BMC Syst. Biol. *2*, 60.

Ju, Q., and Warner, J.R. (1994). Ribosome synthesis during the growth cycle of Saccharomyces cerevisiae. Yeast *10*, 151–157.

Krebs, H.A., and Eggleston, L.V. (1940). The oxidation of pyruvate in pigeon breast muscle. Biochem. J. *34*, 442–459.

Küenzi, M.T., and Fiechter, A. (1969). Changes in carbohydrate composition and trehalase-activity during the budding cycle of Saccharomyces cerevisiae. Arch. Mikrobiol. *64*, 396–407.

Lemons, J.M.S., Feng, X.J., Bennett, B.D., Legesse-Miller, A., Johnson, E.L., Raitman, I., Pollina, E.A., Rabitz, H.A., Rabinowitz, J.D., and Coller, H.A. (2010). Quiescent fibroblasts exhibit high metabolic activity. PLoS Biol. *8*, e1000514.

Lu, C., Brauer, M.J., and Botstein, D. (2009). Slow growth induces heat-shock resistance in normal and respiratory-deficient yeast. Mol. Biol. Cell *20*, 891–903.

Lunt, S.Y., and Vander Heiden, M.G. (2011). Aerobic glycolysis: meeting the metabolic requirements of cell proliferation. Annu. Rev. Cell Dev. Biol. *27*, 441–464.

MacIsaac, K.D., Wang, T., Gordon, D.B., Gifford, D.K., Stormo, G.D., and Fraenkel, E. (2006). An improved map of conserved regulatory sites for Saccharomyces cerevisiae. BMC Bioinformatics *7*, 113.

McKnight, S.L. (2010). On getting there from here. Science *330*, 1338–1339.

Molenaar, D., van Berlo, R., de Ridder, D., and Teusink, B. (2009). Shifts in growth strategies reflect tradeoffs in cellular economics. Mol. Syst. Biol. *5*, 323.

Monod, J. (1949). The Growth of Bacterial Cultures. Annu. Rev. Microbiol. *3*, 371–394.

Newman, J.R., Ghaemmaghami, S., Ihmels, J., Breslow, D.K., Noble, M., DeRisi, J.L., and Weissman, J.S. (2006). Single-cell proteomic analysis of S. cerevisiae reveals the architecture of biological noise. Nature *441*, 840–846.

Newsholme, E.A., Crabtree, B., and Ardawi, M.S. (1985). The role of high rates of glycolysis and glutamine utilization in rapidly dividing cells. Biosci. Rep. *5*, 393–400.

Pelechano, V., and Pérez-Ortín, J.E. (2010). There is a steady-state transcriptome in exponentially growing yeast cells. Yeast *27*, 413–422.

Pfeiffer, T., Schuster, S., and Bonhoeffer, S. (2001). Cooperation and competition in the evolution of ATP-producing pathways. Science *292*, 504–507.

Portman, M.A. (1994). Measurement of unidirectional $P_i \rightarrow ATP$ flux in lamb myocardium *in vivo*. Biochim. Biophys. Acta *1185*, 221–227.

Pujol-Carrion, N., Belli, G., Herrero, E., Nogues, A., and de la Torre-Ruiz, M.A. (2006). Glutaredoxins Grx3 and Grx4 regulate nuclear localisation of Aft1 and the oxidative stress response in Saccharomyces cerevisiae. J. Cell Sci. *119*, 4554–4564.

Rich, P.R. (2003). The molecular machinery of Keilin's respiratory chain. Biochem. Soc. Trans. *31*, 1095–1105.

Schwanhäusser, B., Busse, D., Li, N., Dittmar, G., Schuchhardt, J., Wolf, J., Chen, W., and Selbach, M. (2011). Global quantification of mammalian gene expression control. Nature *473*, 337–342.

Scott, M., Gunderson, C.W., Mateescu, E.M., Zhang, Z., and Hwa, T. (2010). Interdependence of cell growth and gene expression: origins and consequences. Science *330*, 1099–1102.

Shachrai, I., Zaslaver, A., Alon, U., and Dekel, E. (2010). Cost of unneeded proteins in E. coli is reduced after several generations in exponential growth. Mol. Cell *38*, 758–767.

Sheldon, J.G., Williams, S.P., Fulton, A.M., and Brindle, K.M. (1996). 31P NMR magnetization transfer study of the control of ATP turnover in Saccharomyces cerevisiae. Proc. Natl. Acad. Sci. USA *93*, 6399–6404.

Shlomi, T., Benyamini, T., Gottlieb, E., Sharan, R., and Ruppin, E. (2011). Genome-scale metabolic modeling elucidates the role of proliferative adaptation in causing the Warburg effect. PLoS Comput. Biol. *7*, e1002018.

Silverman, S.J., Petti, A.A., Slavov, N., Parsons, L., Briehof, R., Thiberge, S.Y., Zenklusen, D., Gandhi, S.J., Larson, D.R., Singer, R.H., and Botstein, D. (2010). Metabolic cycling in single yeast cells from unsynchronized steady-state populations limited on glucose or phosphate. Proc. Natl. Acad. Sci. USA *107*, 6946–6951.

Slavov, N., and Botstein, D. (2011). Coupling among growth rate response, metabolic cycle, and cell division cycle in yeast. Mol. Biol. Cell *22*, 1997–2009.

Slavov, N., and Botstein, D. (2013). Decoupling nutrient signaling from growth rate causes aerobic glycolysis and deregulation of cell size and gene expression. Mol. Biol. Cell *24*, 157–168.

Slavov, N., Macinskas, J., Caudy, A., and Botstein, D. (2011). Metabolic cycling without cell division cycling in respiring yeast. Proc. Natl. Acad. Sci. USA *108*, 19090–19095.

Slavov, N., Airoldi, E.M., van Oudenaarden, A., and Botstein, D. (2012). A conserved cell growth cycle can account for the environmental stress responses of divergent eukaryotes. Mol. Biol. Cell *23*, 1986–1997.

Slavov, N., Carey, J., and Linse, S. (2013). Calmodulin transduces Ca2+ oscillations into differential regulation of its target proteins. ACS Chem. Neurosci. *4*, 601–612.

Van Hoek, P., Van Dijken, J.P., and Pronk, J.T. (1998). Effect of specific growth rate on fermentative capacity of baker's yeast. Appl. Environ. Microbiol. *64*, 4226–4233.

Van Hoek, P., van Dijken, J.P., and Pronk, J.T. (2000). Regulation of fermentative capacity and levels of glycolytic enzymes in chemostat cultures of Saccharomyces cerevisiae. Enzyme Microb. Technol. *26*, 724–736.

Vander Heiden, M.G., Cantley, L.C., and Thompson, C.B. (2009). Understanding the Warburg effect: the metabolic requirements of cell proliferation. Science *324*, 1029–1033.

Vazquez, A., Liu, J., Zhou, Y., and Oltvai, Z.N. (2010). Catabolic efficiency of aerobic glycolysis: the Warburg effect revisited. BMC Syst. Biol. *4*, 58.

Verduyn, C., Stouthamer, A.H., Scheffers, W.A., and van Dijken, J.P. (1991). A theoretical evaluation of growth yields of yeasts. Antonie van Leeuwenhoek *59*, 49–63.

von Meyenburg, K.H. (1969). Energetics of the budding cycle of *Saccharomyces cerevisiae* during glucose limited aerobic growth. Arch. Mikrobiol. *66*, 289–303.

Warburg, O. (1956). On respiratory impairment in cancer cells. Science *124*, 269–270.

Ward, P.S., and Thompson, C.B. (2012). Metabolic reprogramming: a cancer hallmark even warburg did not anticipate. Cancer Cell *21*, 297–308.

Wiebe, M.G., Rintala, E., Tamminen, A., Simolin, H., Salusjärvi, L., Toivari, M., Kokkonen, J.T., Kiuru, J., Ketola, R.A., Jouhten, P., et al. (2008). Central carbon metabolism of Saccharomyces cerevisiae in anaerobic, oxygen-limited and fully aerobic steady-state conditions and following a shift to anaerobic conditions. FEMS Yeast Res. *8*, 140–154.

Youk, H., and van Oudenaarden, A. (2009). Growth landscape formed by perception and import of glucose in yeast. Nature *462*, 875–879.

Zakrzewska, A., van Eikenhorst, G., Burggraaff, J.E., Vis, D.J., Hoefsloot, H., Delneri, D., Oliver, S.G., Brul, S., and Smits, G.J. (2011). Genome-wide analysis of yeast stress survival and tolerance acquisition to analyze the central trade-off between growth rate and cellular robustness. Mol. Biol. Cell *22*, 4435–4446.

Zampar, G.G., Kümmel, A., Ewald, J., Jol, S., Niebel, B., Picotti, P., Aebersold, R., Sauer, U., Zamboni, N., and Heinemann, M. (2013). Temporal system-level organization of the switch from glycolytic to gluconeogenic operation in yeast. Mol. Syst. Biol. *9*, 651.